1 **Measurement Report: Polycyclic aromatic hydrocarbons (PAHs) and their**

2 **alkylated (RPAHs), nitrated (NPAHs) and oxygenated (OPAHs) derivatives in**

3 **the global marine atmosphere: occurrence, spatial variations, and source**

4 **apportionment**

5 Rui Li[a, b, *, 1], Xing Liu[c, 1], Yubing Shen[a], Yumeng Shao[a], Yining Gao[a], Ziwei Yao[c], Xi Liu[d], Guitao

6 Shi[a,*]

7 [a] *Key Laboratory of Geographic Information Science of the Ministry of Education, School of*

8 *Geographic Sciences, East China Normal University, Shanghai, 200241, PR China*

9 [b] *Institute of Eco-Chongming (IEC), 20 Cuiniao Road, Chenjia Town, Chongming District,*

10 *Shanghai, 202162, China*

11 [c] *State Environmental Protection Key Laboratory of Coastal Ecosystem, National Marine*

12 *Environmental Monitoring Center, Dalian 116023, China*

13 [d] *Agilent Technologies (China) Ltd., Inc., Beijing, 100102, China*

14 *** Corresponding author**

15 Prof. Li (rli@geo.ecnu.edu.cn) and Prof. Shi (gtshi@geo.ecnu.edu.cn)

16 [1]Rui Li and Xing Liu contributed to the work equally.

17 **Abstract**

18 Ambient polycyclic aromatic hydrocarbons (PAHs) and their derivatives have severe adverse

19 impacts on organism health and ecosystem safety. However, their global distributions, sources, and

20 fate in marine aerosol remain poorly understood. To fill the knowledge gap, high-volume air samples

21 were collected along a transect from China to Antarctica and analyzed for particulate PAHs and

22 derivatives. The highest PAH concentrations in marine aerosols were observed in the Western

23 Pacific (WP: 447±228 pg/m³), followed by the East China Sea (ECS: 195 pg/m³), Antarctica Ocean

24 (AO: 111±91 pg/m³), East Australian Sea (EAS: 104±88 pg/m³), and the lowest in the Bismarck Sea

25 (BS: 17±12 pg/m³). Unexpectedly, PAH concentrations in the AO were even higher than those in

26 the EAS and BS. This could be attributed to the relatively low anthropogenic PAH emissions from

27 Australia and Papua New Guinea, whereas AO is often affected by emissions from engine

28 combustion and biomass burning. In contrast to the distribution of PAHs, OPAH levels in the EAS

29 were much higher than those in the AO. It was assumed that OPAHs mainly originated from the

30 secondary formation of parent PAHs through reactions with O_3 and OH radicals, both of which are

31 more prevalent in EAS. Several source apportionment models suggested that PAHs and their

32 derivatives in marine aerosol are dominated by three sources: coal burning and engine combustion

33 emissions (56%), wood and biomass burning (30%), and secondary formation (14%). Specifically,

34 marine aerosols in ECS and WP were significantly affected by coal burning and engine combustion,

35 while those in BS and EAS were mainly influenced by wildfire and coal combustion. AO was

36 primarily dominated by biomass burning and local shipping emissions.

1. Introduction

38   Polycyclic aromatic hydrocarbons (PAHs), a class of semi-volatile organic compounds

39 (SVOCs), are often considered carcinogenic and mutagenic pollutants (Li et al., 2023; Wei et al.,

40 2021). These pollutants are generally released from the combustion of fossil fuels, biofuels, oil spills,

41 and other biogenic sources (Li et al., 2021a; Zhang et al., 2023). Due to long-range atmospheric

42 transport (LRAT), PAHs emitted from industrial and residential sources can often be transported to

43 remote regions such as the open ocean and polar areas (Li et al., 2021a; Zhang et al., 2023). These

44 PAHs species can exert toxic effects on marine organisms through dry and wet deposition (Li et al.,

45 2021b). Additionally, high levels of oxidants (OH radicals, NO_3 radicals, and O_3) enriched in the

46 atmosphere can promote the transformation of parent PAHs into their derivatives (RPAHs, NPAHs,

47 and OPAHs) (Zimmermann et al., 2013). Compared to parent PAHs, nearly all of these derivatives

48 exhibit higher toxic potency to aquatic animals due to their direct-acting mutagenicity (Bandowe

49 and Meusel, 2017; Kovacic and Somanathan, 2014). Therefore, it is crucial to investigate the

50 ~~spatiotemporal~~spatial characteristics of PAHs and their derivatives and to identify the key factors

51 and potential sources of atmospheric PAHs. This knowledge is essential for reducing potential

52 damage to ocean ecosystems and improving marine environmental management.

53   A growing body of literature ~~researches~~ have explored the spatial variations of ambient PAHs

54 in the marine atmosphere. For instance, Kang et al. (2017) found that atmospheric PAH

55 concentrations in the East China Sea ranged from 0.16 to 17.6 ng/m³ (average: 3.87 ng/m³), with

56 these compounds being dominated by 4-ring PAHs. Subsequently, Neroda et al. (2020) investigated

57 PAHs in the aerosols of the North-West Pacific Ocean, estimating total PAH levels ranging from

58 17.1 pg/m³ (northern part of the Sea of Japan) to 142 pg/m³ (La Perouse Strait). More recently,

Wietzoreck et al. (2022) reported that the mean concentrations of total PAHs, RPAHs, OPAHs, and NPAHs in the gas and particulate phases in the Mediterranean were $2.99 \pm 3.35 \, \text{ng/m}^3$, $0.83 \pm 0.87 \, \text{ng/m}^3$, $0.24 \pm 0.25 \, \text{ng/m}^3$, and $4.34 \pm 7.37 \, \text{pg/m}^3$, respectively. Most current studies about PAHs in marine aerosols focus on regional scales, particularly in oceans ~~seas~~ with ~~dense~~ intense anthropogenic activities, while few studies reveal the spatial distributions of PAHs and their derivatives in remote oceans (e.g., the polar oceans) or on a global scale. The Southern Ocean is often considered a remote and pristine sea, and its local ecosystem is more sensitive to PAHs and their derivatives. However, to date, only a few studies have investigated the spatial variations of ambient PAHs in the marine aerosol within this region. Cabrerizo et al. (2014) first demonstrated that the volatilization ~~of~~ from soils and snow~~s~~ might be the major sources of ambient PAHs in the Southern Ocean and Antarctica. Very recently, Overmeiren et al. (2024) analyzed the components of PAHs and OPAHs at a coastal site in Antarctica and found that phenanthrene, pyrene, and fluoranthene derived from volcanic emissions accounted for the major fractions of PAHs. To the best of our knowledge, only Zhang et al. (2022) investigated the global variations of PAH components in marine aerosols and found a clear latitudinal gradient from the Western Pacific to the Southern Ocean. They also identified coal combustion as the major contributor to ambient PAHs (52%). Zetterdahl et al. (2016) also revealed that the shipping emission might play an important role on the PAHs in the marine atmosphere. They verified the new regulation (since late 2014) about the use of low-sulfur residual marine fuel oil instead of heavy oil significantly altered the chemical compositions of PAHs (increasing the low-ring components, while decreasing the high-ring components). Unfortunately, nearly all current studies focus solely on PAHs and OPAHs in regional oceans ~~simultaneously~~, whereas no study has comprehensively investigated the spatial variations of particulate PAHs and all their derivatives on a global scale. Moreover, the source contributions of PAH derivatives in different oceans remain unknown. It is ~~highly necessary~~ important to fill the knowledge gaps regarding the compositions, sources, and fate of PAH derivatives in the marine atmosphere on a global scale.

In our study, an expedition research cruise aboard a Chinese research vessel from October 2019 to April 2020, traveling from China to Antarctica, provided a unique opportunity to reveal the distributions, compositions, and fate of parent PAHs and their derivatives (RPAHs, NPAHs, and

88 OPAHs). Taking advantage of this unique opportunity, our study aims to: (1) investigate the

89 latitudinal gradient of PAHs and their derivatives; (2) study the major factors contributing to the

90 spatial variations; and (3) identify the sources using a Positive Matrix Factorization (PMF) model.

91 **2. Material and methods**

92 2.1 The shipping cruise and sample collection

93 The expedition research cruise of Chinese research vessel took place from October 22 in 2019

94 to April 21 in 2020. The expedition sailed from Shanghai in China, crossing Pacific, Indian Ocean,

95 and Southern Ocean and finally arrived at Antarctica. Then, the return route was also from

96 Antarctica to Shanghai, in China. The detailed information of the shipping line route is depicted in

97 Figure S1 and 1.

98 Atmospheric samples were collected using a high-volume air sampler (HVAS, TISCH

99 Environmental, USA), positioned on the upper deck of the RV/Xuelong, approximately 30 m above

100 sea level. Aerosol particles were captured on Whatman quartz fiber filters (QM-A, 20.3 cm × 25.4

101 cm, pore size 2.5 μm), which were pre-baked at around 500 °C for over 4 hours to eliminate water

102 and organic residues. The HVAS operated at an airflow rate of approximately 1.2 m³ min⁻¹, with

103 each sampling event lasting 2 to 3 days, resulting in total air volumes typically ranging from 3000

104 to 4000 m³. During this time, atmospheric particles were collected along the cruise path, spanning

105 approximately 2 to 4 degrees of latitude, yielding a single aggregate sample per filter. To minimize

106 potential contamination from the research vessel, a wind direction sensor directed the HVAS,

107 ensuring that only air masses from a sector of approximately 120° on either side of the vessel's

108 central trajectory were sampled. After collection, individual filters were carefully separated, folded,

109 wrapped in aluminum foil, placed in zip-lock bags, and stored in the dark at -20 °C until particle

110 characterization analyses began. A total of 35 samples were collected during the cruise, along with

111 2 field blank samples prepared from filters mounted in the HVAS with an air pump flow rate set to

112 0. The sampling protocols for the blanks mirrored those described above regarding duration, filter

113 mounting, collection, transport, observation, and measurements.

114 2.2 Chemical analysis

115 Automated Soxhlet extraction with DCM (JT Baker, Avantor group, Poland), pesticide residue

116 grade) in a B-811 extraction unit (Büchi, Flawil, Switzerland) for PAH, NPAH, and OPAH analysis

117 was employed. The extract was cleaned up using a silica column (with 1 cm i.d. as open tube using

118 5 g of silica (Merck, Darmstadt, Germany), 0.063-0.200 mm, activated at 150 °C for 12 h, 10%

119 deactivated with water) and 1 g Na$_2$SO$_4$ (Merck, Darmstadt, Germany). For the analysis of RPAHs,

120 PM$_{2.5}$ samples were extracted based on the procedure described in Iakovides et al. (2021). A gas

121 chromatograph (Agilent 7890B GC) coupled with the mass spectrometer (Agilent 5977B MS) was

122 employed to determine the concentrations of PAH, NPAH, and OPAH species. The detailed analysis

123 method and quality control of these PAHs and their derivatives are introduced in the supporting

124 information (Text S1 and Table S1). The reference standards of PAHs (Pyr-d10 and BaP-d12; Wako

125 Pure Chemicals, Osaka, Japan), OPAHs (purchased from First Standard (Sigma, America), RPAHs

126 (AccuStandard (New Haven, CT, USA)), and NPAHs (2-fluoro-7-nitrofluorene; Aldrich Chemical

127 Company, Osaka, Japan) were used for calibrating quantification.

128 2.3 Source apportionment

129 As a typical receptor-based model used for source apportionment, the PMF 5.0 version have

130 been widely applied to determine the potential origins of PAH and their derivatives, and to determine

131 the contribution ratios of multiple sources to these components (Sharma et al., 2016). The aim of

132 PMF model is to solve the issues of chemical mass balance between the observed concentration of

133 each PAH species and their source contributions via decomposing the input matrix into factor

134 contributions and factor profiles. The detailed equation is shown in Eq. (1). Additionally, the

135 contribution of each source for an individual component should be ensured to be non-negative.

136 Briefly, the basic principle of PMF is to determine the least object function Q when the g_{ik} must be

137 a non-negative matrix based on Eq. (2) (Jaeckels et al., 2007; Taghvaee et al., 2018).

138
$$x_{ij} = \sum_{k=1}^{p} g_{il} f_{lj} + e_{ij} \quad (1)$$

139
$$Q = \sum_{i=1}^{n} \sum_{j=1}^{m} [\frac{x_{ij} - \sum_{k=1}^{p} g_{il} f_{lj}}{u_{ij}}]^2 \quad (2)$$

140 where x_{ij} and e_{ij} represent the PAH concentrations and uncertainty of the jth component, respectively.

141 g_{il} denotes the contribution ratio of the lth source to the ith sample, f_{lj} is the ratio of the jth component

142 in the lth source, and e_{ij} denotes the residual of the jth element in the ith sample. The 2-6 factor

143 solutions were examined, and a three-factor solution was decided with the ratio of Q (robust) and Q

144 (true) reaching 0.93. The coefficients of determination (R_s^2) between the predicted and observed

145 concentrations of PAHs and their derivatives were shown in Table S2. The uncertainties linked with

146 factor profiles were assessed based on three error calculation methods including the bootstrap (BS)

147 method, displacement (DISP) analysis, and the combination method of DISP and BS (BS-DISP).

148 For the BS method, 1000 runs were conducted and the result has been considered to be robust

149 because all of the factors showed a mapping of above 90%. DISP analysis also demonstrated that

150 this solution was stable because the observed drop in the Q value was < 0.1% and no factor swap

151 occurred. For the BS-DISP analysis, the solution has been verified to be useful because the observed

152 drop in the Q value was < 0.5%. Moreover, both of the results from BS and BS-DISP did not show

153 any asymmetry or rotational ambiguity for all of the factors (Ambade et al., 2023; Gao et al., 2015;

154 Yan et al., 2017).

155 2.4 GEOS-Chem model

156 GEOS-Chem (v13.4.0) model was employed to estimate O_3 and OH radical concentrations

157 during Jan. 1-Dec. 31 in 2019. This model comprises of a complex chemistry mechanism of

158 tropospheric NO_x-VOC-O_3-aerosol (Park et al., 2004). This model was driven by MERRA2

159 meteorological parameters (Hamal et al., 2020; Koster et al., 2020; Qiu et al., 2020). A global

160 simulation was conducted at a spatial resolution of 2 × 2.5° resolution (Qiu et al., 2020; Weagle et

161 al., 2018; Zhang et al., 2021a). The historical multi-sector anthropogenic emission dataset was

162 downloaded from Community Emissions Data System (Hoesly et al., 2018). Natural emissions

163 including wildfire, soil emission, and lightning emissions were also incorporated into the GEOS-

164 Chem model. Wildfire emissions derived from Global Fire Emissions Database (GFED) were used

165 for simulations (Chen et al., 2023). The lightning NO_X emission was collected from

166 http://geoschemdata.wustl.edu/ExtData/HEMCO/OFFLINE_LIGHTNING/v2020-03/MERRA2/

167 (Murray et al., 2012).

168 **3 Results and discussions**

169 3.1 The chemical compositions of PAHs and their derivatives in the atmosphere

170 The concentrations of 18 PAHs, 11 OPAHs, 9 RPAHs, and 7 NPAHs in 33 samples were

171 determined. The average concentrations of ΣPAHs, ΣOPAHs, ΣRPAHs, and ΣNPAHs were 157±98,

172 1920±1250, 12.1±9.5, and 3.0±1.6 pg/m^3, respectively. The total concentrations of PAHs and their

173 derivatives in the marine aerosols (Pacific and Antarctic Ocean (AO)) were significantly lower than

174 those in urban regions such as Harbin (86.9 ng/m^3) (Ma et al., 2020), Augsburg (1.3 ng/m^3)

175 (Pietrogrande et al., 2011), and Southeastern Florida (3.0 ng/m^3) (Sevimoglu and Rogge, 2016).

176 However, the PAHs concentration in our study was comparable to those in some remote regions.

177 For instance, Cabrerizo et al. (2014) found that the total concentration of 18 particulate PAHs over

178 AO ranged from 0.03 to 4.2 ng/m^3. Later on, Zhang et al. (2022) reported that the 15 PAHs in PM$_{2.5}$

179 across Pacific and AO ranged from 0.11 to 1.2 ng/m^3. Very recently, Van Overmeiren et al. (2024)

180 revealed that the total concentrations of 15 PAHs in PM$_{2.5}$ in Antarctica was only 1.5 pg/m^3, which

181 was even much lower than the result in our study. The large gaps for PAH concentrations between

182 remote ocean (polar region) and urban regions might be associated with the intensity of

183 anthropogenic emission (Shen et al., 2013; Zhang and Tao, 2009). Although the total concentration

184 could provide the overall picture of PAHs in the global marine boundary layer, the specific

185 compounds in PAHs also varied greatly.

186   Among all of the PAHs, the BbF showed the highest level (26.8±10.4 pg/m^3), followed by Ace

187 (18.4±9.8 pg/m^3), Fluoran (16.3±8.4 pg/m^3), and the lowest one was Acy (0.12±0.05 pg/m^3) (Figure

188 2). Overall, the PAHs in the global marine aerosols were dominated by 3-5 ring components (~83%),

189 which was in agreement with the result in Pacific and Indian Ocean observed by Zhang et al. (2022).

190 It was reported that Fluoran, Acy, and Ace were often sourced from biomass or coke burning (Zhang

191 et al., 2021c), while BbF was generally enriched in the production of wood and coal combustion (Li

192 et al., 2022), indicating the marine aerosol could be influenced by the solid fuel burning.

193   Among all of the OPAHs, 1-Naphthaldehyd showed the highest concentration (852±406 pg/m^3),

194 followed by 1,4-Chysenequione (787±386 pg/m^3), Ancenaphthenaquinone (133±75 pg/m^3),

195 Anthraquinone (58±31 pg/m^3), and the lowest one was 5,12-Naphthacenequione (1.49±0.64 pg/m^3).

196 In general, the absolute concentrations of OPAHs were comparable or slightly lower than those of

197 PAHs especially in some high-latitude sites. Nevertheless, the OPAHs concentrations in our study

198 were markedly higher than PAHs levels ($p < 0.01$). It was well known that OPAHs was often

199 released from incomplete combustion or generated from photochemical reactions of O$_3$, OH, and

200 NO$_3$ radicals with PAHs (Zhang et al., 2022). The higher concentrations of O$_3$ and OH radicals over

201 tropical oceans might largely promote the PAH oxidation (Zhang et al., 2022). For RPAHs, 1,3-

202 Dimethylnaphthalene (4.47±2.64 pg/m^3) and 2-Methylnaphthalene (4.38±2.42 pg/m^3) accounted for

203 the major fractions (73%) of RPAHs, while the concentrations of other species were relatively low.

204 Wietzoreck et al. (2022) confirmed the chemical compositions of RPAHs in Middle East Seas

205 displayed similar patterns with our study. The NPAHs in the marine aerosol were also dominated by

206 2-Nitronaphthalene (2.2±1.1 pg/m^3) and 5-Nitroacenaphthene (2.0±0.7 pg/m^3), while the

207 contributions of other species were negligible.

208 3.2 The spatial variations of particulate PAHs derivatives and key meteorological factors

209   To reveal the spatial variations of atmospheric PAHs and the derivatives, all of the sampling

210 sites were divided into five groups (regions): East China Sea (ECS), Western Pacific (WP),

211 Bismarck Sea (BS), Eastern Australia Sea (EAS), and AO. The PAHs concentrations followed the

212 order of WP (447±228 pg/m^3) > ECS (195 pg/m^3) > AO (111±91 pg/m^3) > EAS (104±88 pg/m^3) >

213 BS (17±12 pg/m^3) (Figure 3). Based on Mann-Whitney test, the PAHs concentrations in WP were

214 significantly higher than those in other oceans ($p < 0.05$). High levels of PAHs in WP are closely

215 linked with the high coverage of continent-affected regions such as Southeast Asian and East Asian

216 countries. AO showed the lower PAHs concentrations because the sea was far away from continental

217 sources. In general, PAH levels in the remote marine atmosphere appear to be affected by long-

218 range transport and air-seawater exchange, whereas local anthropogenic emission might be

219 responsible for the ambient PAHs near the continent. For AO, the Antarctica continent lacks of

220 anthropogenic activity, and thus it leads to the lower PAHs levels in the atmosphere of AO. It should

221 be noted that both of EAS and BS were close to Australia, while the PAHs concentrations in these

222 oceans were even lower than those in AO. It was assumed that Australia possesses very low

223 anthropogenic PAH emission (< 10 μg/km^2) compared with many other continents (Shen et al.,

224 2013). Although the total PAHs showed remarkably higher concentrations in ECS and WP, all of

225 the congeners did not show the same spatial variations with the total PAHs level. For instance,

226 Fluoran, Pyr, BeP, and BaP levels in AO were even higher than those in ECS, ~~–~~and the BbF levels

227 in EAS ~~was~~ were much higher than those in ECS. ~~It was well documented that Pyr, BeP, and BaP~~

228 ~~were mainly derived from engine combustion emissions (Van Overmeiren et al., 2024), indicating~~

229 ~~that the marine aerosols in AO was often influenced by the shipping emission.~~ BbF generally

230 originated from wood burning (Zhang et al., 2022a), and wildfire often occurred in the summer and

231 autumn of Australia (Haque et al., 2021), which might elevate the BbF concentration in the marine

232 aerosol along Australia. The simulated wildfire-related ambient benzene concentration via GEOS-

233 Chem model (Figure S2) was utilized to establish the relationship with the ambient BbF level in the

234 aerosols, and the correlation coefficient reached 0.52 ($p < 0.05$). The result confirmed that local

235 wildfire in Australia largely increased BbF concentration in the marine aerosol.

236   The total OPAHs also exhibited marked spatial variations with the highest concentrations in

237 WP (3328±1846 pg/m^3), followed by EAS (2675±1452 pg/m^3), ECS (2506 pg/m^3), AO (1447±865

238 pg/m^3), and the lowest one in BS (897±544 pg/m^3). Different from the spatial distribution of parent

239 PAHs, OPAHs levels in EAS were much higher than those in AO and BS. It was widely

240 acknowledged that OPAHs were mainly derived from the secondary formation of parent PAH and

241 O_3 and OH radicals (Ambade et al., 2023). It was assumed that both of O_3 and OH radicals were

242 higher in the tropical oceans compared with the temperate and southern oceans based on GEOS-

243 Chem model (Figure S3). The correlation analysis also suggested that the OPAHs concentrations

244 displayed good relationship with O_3 level (r = 0.55, p < 0.05). In addition, the ratios of OPAH/PAH

245 in ECS, WP, BS, EAS, and AO were 13, 7, 53, 26, and 13, respectively. We could find that the

246 oxidation capacities of PAH in BS and EAS were much higher compared with other oceans, though

247 the primary emission of PAH in BS was relatively low. All of these results demonstrated that the

248 strong oxidation capacity of O_3 and OH radical promoted the higher OPAHs concentrations. Most

249 of the OPAH species displayed ~~the~~ similar spatial variations with the total OPAHs concentrations,

250 while few components such as 1-Naphthaldehyd, Ancenaphthenaquinone, and 6H-

251 Benzo(cd)pyrene-6-one levels in ECS were still higher than those in EAS. It might be linked with

252 the emission intensity of their precursors.

253   Both of RPAHs and NPAHs showed the higher levels in ECS (20 and 3.6 pg/m^3) and WP

254 (22±13 and 3.0±1.2 pg/m^3), which were significantly higher than those in other seas. Among all of

255 the species of RPAHs and NPAHs, 1-Methylnaphthalene and 2-Nitronaphthalene exhibited

256 significantly higher concentrations in ECS (1.61 and 3.61 pg/m^3) and WP (2.1±1.3 and 2.8±1.1

257 pg/m^3) compared with other regions (Figure S4 and S5) ($p < 0.05$). It ~~was~~ has been well documented

258 that both of these species were derived from diesel vehicle emission. Southeast Asia and East Asia

259 showed the higher diesel vehicle emission of parent PAHs compared with Australia and some

260 countries in the Southern hemisphere (Shen et al., 2013).

261 Besides, some key meteorological factors including 2-m air temperature (T), 2-m dewpoint

262 temperature (Dew), precipitation (Prec), and wind speed (WS) were also selected to assess their

263 impacts on PAH derivatives (Figure 4). The result suggested that most of PAH derivatives showed

264 significant negative correlation with nearly all of the meteorological parameters. Among all of the

265 meteorological parameters, WS showed the highest correlation coefficients with all of the PAH

266 derivatives, indicating that dilution and diffusion conditions significantly affected their fate because

267 most of these compounds showed relatively long lifetime. Besides, T also showed the higher

268 negative correlation with PAH derivatives because the gas-particle partitioning of PAHs was mainly

269 controlled by the air temperature (Li et al., 2020; Wang et al., 2019b). High air temperature usually

270 suppresses gaseous to particulate sorption of PAH derivatives to marine aerosol, and compound-

271 dependent adsorption kinetics in the atmosphere (Andreae, 1983; Gustafson and Dickhut, 1996;

272 Wang et al., 2019a). Although rainfall washout might be an important pathway for PAH decrease,

273 the correlation coefficients of Prec and PAH derivatives were slightly lower than other

274 meteorological factors. It was assumed that the sampling period showed less rainfall events, and

275 thus the PAH derivatives were not sensitive to Prec. Compared with other PAH derivatives, RPAHs

276 showed low correlation coefficient with meteorological parameters.

277 3.3 Source apportionment of parent PAH and derivatives

278 The diagnostic ratio between PAHs has been widely utilized to identify the major sources of

279 particulate PAHs. Based on previous studies, the Fluoran/(Fluoran +Pyr) ratio could be applied to

280 distinguish the potential sources. The ratios less than 0.4, 0.4-0.5, and greater than 0.5 could be

281 treated to be petrogenic source (0.4), petroleum combustion or biomass burning (0.4-0.5), and the

282 coal combustion (> 0.5), respectively (Yunker et al., 2002; Zhang et al., 2021a). In our study, the

283 Fluoran/(Fluoran +Pyr) ratio in nearly all of the regions except AO (0.46) were higher than 0.5,

284 indicating the impact of coal combustion on marine aerosols in most regions in Northern

285 Hemisphere and tropical regions. The geochemical index method shows some uncertainties, and

286 thus it is necessary to employ more diagnostic ratios to enhance the reliability. BaP/BghiP ratio was

287 also widely applied to separate the sources of vehicle emission (≤ 0.6) and coal burning (> 0.6).

288 Both of BS (0.90) and EAS (0.84) showed the higher BaP/BghiP ratios, indicating the important

289   impact of coal combustion on the local marine aerosol (Katsoyiannis et al., 2007). However, the

290   ratio in ECS was much lower than 0.6, indicating that the vehicle or shipping emission also plays a

291   ~~unignorable~~ significant role on the local aerosol. Meanwhile, the BaP/(BaP+CT) ratios in ECS and

292   WP reached 0.09 and 0.31, respectively. The result fills in the domain derived from diesel emission,

293   which further supported the inference that the marine aerosols in both of ECS and WP were

294   significantly affected by diesel emission (Ma et al., 2020). For AO, all of the diagnostic ratios

295   suggested that the oceans were mainly affected by shipping emission and wood burning.

296   Although the geochemical index method could identify the potential sources of PAH species,

297   the contributions of multiple sources to PAHs and their derivatives still remained unknown.

298   Therefore, positive matrix factorization (version PMF 5.0) was utilized to determine more source

299   information of PAH species. After 30 runs, the optimal three factors with the lowest values of Q

300   (robust) and Q (true) were determined. Factor 1 (56%) possesses the higher loadings of Fluoran,

301   BaA, CT, BeP, BaP, and 1-Methylnaphthalene (Figure 5). It was well known that Fluoran and BaA

302   were typical indicators for coal combustion (Wang et al., 2016). Meanwhile, BeP, BaP, and 1-

303   Methylnaphthalene were often derived from shipping emission (Li et al., 2022). Therefore, factor 1

304   could be defined as the mixed source of coal burning and engine combustion emission. Factor 2

305   (30%) shows a high correlation with LMW PAHs such as Nap, Flu, Phe, Ant, BbF. It was well

306   documented that these LMW PAH species mainly originated from wood and biomass burning (Chen

307   et al., 2022; Zhang et al., 2021a; Zhang et al., 2020). Factor 3 (14%) is characterized by medium

308   and high contributions of 5,12-Naphthacenequione, 1,6,7-Trimethylnaphthalene, and 2-

309   Nitronaphthalene. Many previous studies have confirmed that the photochemical reaction involving

310   NO_2 initiated by OH radicals was highly effective for the production of 2-Nitronaphthalene in $PM_{2.5}$

311   (Arey et al., 1990; Atkinson et al., 1990). Hence, the factor could be treated to be the secondary

312   formation. Based on the source apportionment, we verified that EAS showed relatively high

313   secondary contribution compared with some regions such ECS and WP. It was assumed that EAS

314   showed the higher atmospheric oxidates and low PAH emissions (Ambade et al., 2023; Shen et al.,

315   2013), which was in good agreement the spatial variations of PAHs and OPAHs.

316   **4   Conclusions and implications**

317   In summary, our study verifies the ubiquitous occurrence of PAHs and their derivatives in the

318 aerosols of the Western Pacific (WP), Bismarck Sea (BS), East Australian Sea (EAS), and even the

319 Antarctica Ocean (AO). The highest PAH concentrations in marine aerosols were observed in WP

320 (447 ± 228 pg/m³), followed by the East China Sea (ECS) (195 pg/m³), AO (111 ± 91 pg/m³), EAS

321 (104 ± 88 pg/m³), and the lowest in BS (17 ± 12 pg/m³). PAH derivatives (e.g., OPAHs, RPAHs, and

322 NPAHs) also showed higher concentrations in WP. The spatial characteristics of these components

323 can be related to precursor emissions and oxidation patterns (e.g., OH/NO$_3$ radicals, O$_3$).

324 For instance, the higher PAH and derivative concentrations observed in WP were primarily due

325 to higher anthropogenic emissions from coal and engine combustion. PAH concentrations in AO

326 were even higher than those in EAS and BS, while OPAH levels in EAS were much higher than

327 those in AO. It is widely acknowledged that OPAHs mainly originate from the secondary formation

328 of parent PAHs through reactions with O$_3$ and OH radicals. The concentrations of O$_3$ and OH

329 radicals are higher in tropical oceans compared to temperate and southern oceans.

330 Both of geochemical index methods and the PMF model suggested that PAHs and their

331 derivatives in global marine aerosols are controlled by three major sources: coal burning and engine

332 combustion emissions (56%), wood and biomass burning (30%), and secondary formation (14%).

333 Marine aerosols in ECS and WP were dominated by coal burning and engine combustion, while BS

334 and EAS were mainly influenced by wildfires and coal combustion. AO was significantly affected

335 by biomass burning and local shipping emissions.

336 However, this study has some limitations. Firstly, it focuses only on particle-phase PAHs and

337 derivatives, while gas-phase PAH species were not measured. Additionally, data on PAHs in

338 seawater were lacking. Future research should investigate gas-particle partitioning and the exchange

339 processes between air and seawater phases in the global marine environment. Moreover, our study

340 did not include cruise observations of marine aerosols in the Atlantic and Arctic Oceans. Future

341 studies should collect marine aerosols from all major oceans. Furthermore, measuring the

342 concentrations of PAHs and derivatives in marine aerosols over multiple years will help analyze the

343 impact of changes in anthropogenic emissions on these components, providing insight into their

344 spatial distribution and fate (formation or removal mechanisms).

345 **Acknowledgements**

346 This work was supported by the National Natural Science Foundation of China (42107113,

347 42276243), and the Fundamental Research Funds for the Central Universities. The authors are

348 grateful to the CHINARE members for their support and assistance in atmosphere sampling.

349 **Data Availability Statement**

350 The data presented in this study are available at the Zenodo data archive

351 https://zenodo.org/records/14291911 (Li et al., 2024).

352 **Author Contributions**

353 Conceptualization: Rui Li, Xing Liu, and Guitao Shi; Data Curation: Yubing Shen, Yumeng Shao,

354 and Yining Gao; Formal analysis: Ziwei Yao, Qian Liu

355 **Competing interests**

356 The contact author has declared that none of the authors has any competing interests.

357

References

358   Ambade, B., Sethi, S.S., Chintalacheruvu, M.R. (2023) Distribution, risk assessment, and source apportionment of polycyclic aromatic hydrocarbons (PAHs) using positive matrix factorization (PMF) in urban soils of East India. Environmental geochemistry and health 45, 491-505.

Andreae, M.O. (1983) Soot carbon and excess fine potassium: Long-range transport of combustion-derived aerosols. Science 220, 1148-1151.

Arey, J., Atkinson, R., Aschmann, S.M., Schuetzle, D. (1990) Experimental investigation of the atmospheric chemistry of 2-methyl-1-nitronaphthalene and a comparison of predicted nitroarene concentrations with ambient air data. Polycyclic Aromatic Compounds 1, 33-50.

Atkinson, R., Arey, J., Zielinska, B., Aschmann, S.M. (1990) Kinetics and nitro-products of the gas-phase OH and NO3 radical-initiated reactions of naphthalene-d8, Fluoranthene-d10, and pyrene. International Journal of Chemical Kinetics 22, 999-1014.

Bandowe, B.A.M., Meusel, H. (2017) Nitrated polycyclic aromatic hydrocarbons (nitro-PAHs) in the environment–a review. Science of the Total Environment 581, 237-257.

Cabrerizo, A., Galbán-Malagón, C., Del Vento, S., Dachs, J. (2014) Sources and fate of polycyclic aromatic hydrocarbons in the Antarctica and Southern Ocean atmosphere. Global Biogeochemical Cycles 28, 1424-1436.

Chen, Y.-P., Zeng, Y., Guan, Y.-F., Huang, Y.-Q., Liu, Z., Xiang, K., Sun, Y.-X., Chen, S.-J. (2022) Particle size-resolved emission characteristics of complex polycyclic aromatic hydrocarbon (PAH) mixtures from various combustion sources. Environmental Research 214, 113840.

Gao, B., Wang, X.-M., Zhao, X.-Y., Ding, X., Fu, X.-X., Zhang, Y.-L., He, Q.-F., Zhang, Z., Liu, T.-Y., Huang, Z.-Z. (2015) Source apportionment of atmospheric PAHs and their toxicity using PMF: Impact of gas/particle partitioning. Atmospheric Environment 103, 114-120.

Gustafson, K.E., Dickhut, R.M. (1996) Particle/gas concentrations and distributions of PAHs in the atmosphere of southern Chesapeake Bay. Environmental science & technology 31, 140-147.

Haque, M.K., Azad, M.A.K., Hossain, M.Y., Ahmed, T., Uddin, M., Hossain, M.M. (2021) Wildfire in Australia during 2019-2020, Its impact on health, biodiversity and environment with some proposals for risk management: a review. Journal of Environmental Protection 12, 391-414.

387   Jaeckels, J.M., Bae, M.-S., Schauer, J.J. (2007) Positive matrix factorization (PMF) analysis of

388 molecular marker measurements to quantify the sources of organic aerosols. Environmental science

389 & technology 41, 5763-5769.

390   Kang, M., Yang, F., Ren, H., Zhao, W., Zhao, Y., Li, L., Yan, Y., Zhang, Y., Lai, S., Zhang, Y.

391 (2017) Influence of continental organic aerosols to the marine atmosphere over the East China Sea:

392 Insights from lipids, PAHs and phthalates. Science of the Total Environment 607, 339-350.

393   Katsoyiannis, A., Terzi, E., Cai, Q.-Y. (2007) On the use of PAH molecular diagnostic ratios in

394 sewage sludge for the understanding of the PAH sources. Is this use appropriate? Chemosphere 69,

395 1337-1339.

396   Kovacic, P., Somanathan, R. (2014) Nitroaromatic compounds: Environmental toxicity,

397 carcinogenicity, mutagenicity, therapy and mechanism. Journal of Applied Toxicology 34, 810-824.

398   Li, B., Zhou, S., Wang, T., Zhou, Y., Ge, L., Liao, H. (2020) Spatio-temporal distribution and

399 influencing factors of atmospheric polycyclic aromatic hydrocarbons in the Yangtze River Delta.

400 Journal of Cleaner Production 267, 122049.

401   Li, C., Li, Z., Wang, H. (2023) Characterization and risk assessment of polycyclic aromatic

402 hydrocarbons (PAHs) pollution in particulate matter in rural residential environments in China-A

403 review. Sustainable Cities and Society, 104690.

404   Li, D., Zhao, Y., Du, W., Zhang, Y., Chen, Y., Lei, Y., Wu, C., Wang, G. (2022) Characterization

405 of PM2. 5-bound parent and oxygenated PAHs in three cities under the implementation of Clean Air

406 Action in Northern China. Atmospheric Research 267, 105932.

407   Li, R., Hua, P., Krebs, P. (2021a) Global trends and drivers in consumption-and income-based

408 emissions of polycyclic aromatic hydrocarbons. Environmental science & technology 56, 131-144.

409   Li, R., Shen, Y., Shao, Y., Gao, Y., Yao, Z., Liu, Q., Liu, X., Shi, G. (2024) Measurement Report:

410 Polycyclic aromatic hydrocarbons (PAHs) and their alkylated (RPAHs), nitrated (NPAHs) and

411 oxygenated (OPAHs) derivatives in the global marine atmosphere: occurrence, spatial variations,

412 and source apportionment. Atmospheric Chemistry and Physics.

413   Li, Y., Liu, M., Hou, L., Li, X., Yin, G., Sun, P., Yang, J., Wei, X., He, Y., Zheng, D. (2021b)

414 Geographical distribution of polycyclic aromatic hydrocarbons in estuarine sediments over China:

415 Human impacts and source apportionment. Science of the Total Environment 768, 145279.

416 Lian, L., Huang, T., Ke, X., Ling, Z., Jiang, W., Wang, Z., Song, S., Li, J., Zhao, Y., Gao, H.

417 (2021) Globalization-driven industry relocation significantly reduces arctic PAH contamination.

418 Environmental science & technology 56, 145-154.

419 Ma, L., Li, B., Liu, Y., Sun, X., Fu, D., Sun, S., Thapa, S., Geng, J., Qi, H., Zhang, A. (2020)

420 Characterization, sources and risk assessment of PM2. 5-bound polycyclic aromatic hydrocarbons

421 (PAHs) and nitrated PAHs (NPAHs) in Harbin, a cold city in Northern China. Journal of Cleaner

422 Production 264, 121673.

423 Neroda, A.S., Goncharova, A.A., Mishukov, V.F. (2020) PAHs in the atmospheric aerosols and

424 seawater in the North–West Pacific Ocean and Sea of Japan. Atmospheric Environment 222, 117117.

425 Pegoraro, C.N., Quiroga, S.L., Montejano, H.A., Rimondino, G.N., Argüello, G.A., Chiappero,

426 M.S. (2020) Assessing polycyclic aromatic hydrocarbons in the marine atmosphere on a transect

427 across the Southwest Atlantic Ocean. Atmospheric Pollution Research 11, 1035-1041.

428 Pietrogrande, M.C., Abbaszade, G., Schnelle-Kreis, J., Bacco, D., Mercuriali, M.,

429 Zimmermann, R. (2011) Seasonal variation and source estimation of organic compounds in urban

430 aerosol of Augsburg, Germany. Environmental pollution 159, 1861-1868.

431 Sevimoglu, O., Rogge, W.F. (2016) Seasonal size-segregated PM10 and PAH concentrations

432 in a rural area of sugarcane agriculture versus a coastal urban area in Southeastern Florida, USA.

433 Particuology 28, 52-59.

434 Sharma, S., Mandal, T., Jain, S., Saraswati, Sharma, A., Saxena, M. (2016) Source

435 apportionment of PM$_{2.5}$ in Delhi, India using PMF model. Bulletin of environmental contamination

436 and toxicology 97, 286-293.

437 Shen, H., Huang, Y., Wang, R., Zhu, D., Li, W., Shen, G., Wang, B., Zhang, Y., Chen, Y., Lu,

438 Y. (2013) Global atmospheric emissions of polycyclic aromatic hydrocarbons from 1960 to 2008

439 and future predictions. Environmental science & technology 47, 6415-6424.

440 Taghvaee, S., Sowlat, M.H., Mousavi, A., Hassanvand, M.S., Yunesian, M., Naddafi, K.,

441 Sioutas, C. (2018) Source apportionment of ambient PM2. 5 in two locations in central Tehran using

442 the Positive Matrix Factorization (PMF) model. Science of the Total Environment 628, 672-686.

443 Van Overmeiren, P., Demeestere, K., De Wispelaere, P., Gili, S., Mangold, A., De Causmaecker,

444 K., Mattielli, N., Delcloo, A., Langenhove, H.V., Walgraeve, C. (2024) Four Years of Active

Sampling and Measurement of Atmospheric Polycyclic Aromatic Hydrocarbons and Oxygenated Polycyclic Aromatic Hydrocarbons in Dronning Maud Land, East Antarctica. Environmental science & technology 58, 1577-1588.

Wang, J., Ho, S.S.H., Huang, R., Gao, M., Liu, S., Zhao, S., Cao, J., Wang, G., Shen, Z., Han, Y. (2016) Characterization of parent and oxygenated-polycyclic aromatic hydrocarbons (PAHs) in Xiʹan, China during heating period: An investigation of spatial distribution and transformation. Chemosphere 159, 367-377.

Wang, L., Dong, S., Liu, M., Tao, W., Xiao, B., Zhang, S., Zhang, P., Li, X. (2019a) Polycyclic aromatic hydrocarbons in atmospheric PM2. 5 and PM10 in the semi-arid city of Xi'an, Northwest China: Seasonal variations, sources, health risks, and relationships with meteorological factors. Atmospheric Research 229, 60-73.

Wang, Y., Zhang, Q., Zhang, Y., Zhao, H., Tan, F., Wu, X., Chen, J. (2019b) Source apportionment of polycyclic aromatic hydrocarbons (PAHs) in the air of Dalian, China: Correlations with six criteria air pollutants and meteorological conditions. Chemosphere 216, 516-523.

Wei, C., Bandowe, B.A.M., Han, Y., Cao, J., Watson, J.G., Chow, J.C., Wilcke, W. (2021) Polycyclic aromatic compounds (PAHs, oxygenated PAHs, nitrated PAHs, and azaarenes) in air from four climate zones of China: Occurrence, gas/particle partitioning, and health risks. Science of the Total Environment 786, 147234.

Wietzoreck, M., Kyprianou, M., Musa Bandowe, B.A., Celik, S., Crowley, J.N., Drewnick, F., Eger, P., Friedrich, N., Iakovides, M., Kukučka, P. (2022) Polycyclic aromatic hydrocarbons (PAHs) and their alkylated, nitrated and oxygenated derivatives in the atmosphere over the Mediterranean and Middle East seas. Atmospheric Chemistry and Physics 22, 8739-8766.

Yan, Y., He, Q., Guo, L., Li, H., Zhang, H., Shao, M., Wang, Y. (2017) Source apportionment and toxicity of atmospheric polycyclic aromatic hydrocarbons by PMF: Quantifying the influence of coal usage in Taiyuan, China. Atmospheric Research 193, 50-59.

Yunker, M.B., Macdonald, R.W., Vingarzan, R., Mitchell, R.H., Goyette, D., Sylvestre, S. (2002) PAHs in the Fraser River basin: a critical appraisal of PAH ratios as indicators of PAH source and composition. Organic geochemistry 33, 489-515.

Zetterdahl, M., Moldanova, J., Pei, X.Y., Pathak R.V., Demirdjian, B. (2016) Impact of the 0.1%

fuel sulfur content limit in SECA on particle and gaseous emissions from marine vessels. Atmospheric Environment 145, 338-345.

Zhang, L., Yang, L., Bi, J., Liu, Y., Toriba, A., Hayakawa, K., Nagao, S., Tang, N. (2021a) Characteristics and unique sources of polycyclic aromatic hydrocarbons and nitro-polycyclic aromatic hydrocarbons in $PM_{2.5}$ at a highland background site in northwestern China ☆ . Environmental pollution 274, 116527.

Zhang, L., Yang, L., Zhou, Q., Zhang, X., Xing, W., Wei, Y., Hu, M., Zhao, L., Toriba, A., Hayakawa, K. (2020) Size distribution of particulate polycyclic aromatic hydrocarbons in fresh combustion smoke and ambient air: A review. Journal of Environmental Sciences 88, 370-384.

Zhang, P., Zhou, Y., Chen, Y., Yu, M., Xia, Z. (2023) Construction of an atmospheric PAH emission inventory and health risk assessment in Jiangsu, China. Air Quality, Atmosphere & Health 16, 629-640.

Zhang, R., Han, M., Yu, K., Kang, Y., Wang, Y., Huang, X., Li, J., Yang, Y. (2021b) Distribution, fate and sources of polycyclic aromatic hydrocarbons (PAHs) in atmosphere and surface water of multiple coral reef regions from the South China Sea: A case study in spring-summer. Journal of hazardous materials 412, 125214.

Zhang, X., Zhang, Z.-F., Zhang, X., Zhu, F.-J., Li, Y.-F., Cai, M., Kallenborn, R. (2022a) Polycyclic aromatic hydrocarbons in the marine atmosphere from the Western Pacific to the Southern Ocean: Spatial variability, Gas/particle partitioning, and source apportionment. Environmental science & technology 56, 6253-6261.

Zhang, Y., Shen, Z., Sun, J., Zhang, L., Zhang, B., Zou, H., Zhang, T., Ho, S.S.H., Chang, X., Xu, H. (2021c) Parent, alkylated, oxygenated and nitrated polycyclic aromatic hydrocarbons in PM2. 5 emitted from residential biomass burning and coal combustion: A novel database of 14 heating scenarios. Environmental pollution 268, 115881.

Zhang, Y., Tao, S. (2009) Global atmospheric emission inventory of polycyclic aromatic hydrocarbons (PAHs) for 2004. Atmospheric Environment 43, 812-819.

Zhang, Z.-F., Chen, J.-C., Zhao, Y.-X., Wang, L., Teng, Y.-Q., Cai, M.-H., Zhao, Y.-H., Nikolaev, A., Li, Y.-F. (2022b) Determination of 123 polycyclic aromatic hydrocarbons and their derivatives in atmospheric samples. Chemosphere 296, 134025.

503   Zimmermann, K., Jariyasopit, N., Massey Simonich, S.L., Tao, S., Atkinson, R., Arey, J. (2013)

504   Formation of nitro-PAHs from the heterogeneous reaction of ambient particle-bound PAHs with

505   N2O5/NO3/NO2. Environmental science & technology 47, 8434-8442.

506

507
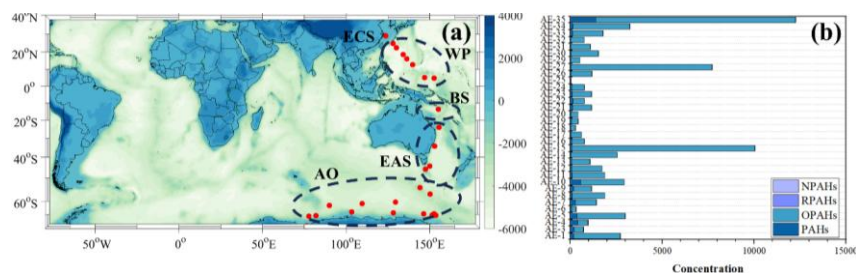
508   **Figure 1** The sampling sites during the cruise from Shanghai to Antarctica (red dots) (a). The total

509   concentrations (Unit: pg/m^3) of PAHs, OPAHs, RPAHs, and NPAHs for all of the samples (from

510   AE-1 to AE-35) (b). The indicators from AE-1 to AE-35 represent the collected aerosol samples in

511   the global marine. ECS, WP, BS, EAS, and AO represent East China Sea, Western Pacific, Bismarck

512   Sea, Eastern Australia Sea, and Antarctic Ocean, respectively.
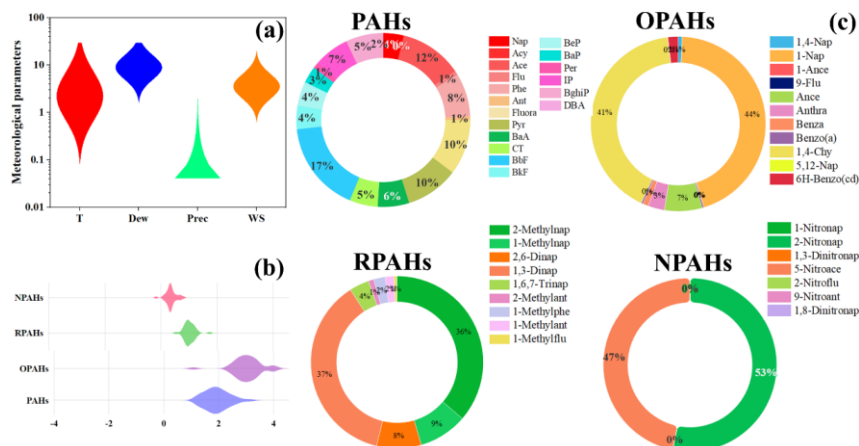
Figure 2 The average meteorological parameters during the cruise (a). T, Dew, Prec, and WS denote

2-m air temperature (Unit: ℃), dewpoint temperature (Unit: ℃), precipitation (mm), and wind

speed (m/s), respectively. The average concentrations (log_{10} (concentration), Unit: pg/m^3) of PAHs,

OPAHs, RPAHs, and NPAHs for all of the samples (b). The contribution ratios of species in PAHs,

OPAHs, RPAHs, and NPAHs (Unit: %) (c). For OPAHs, 1,4-Nap, 1-Nap, 1-Ance, 9-Flu, Ance,

Anthra, Benza, Benzo (a), 1,4-Chy, 5,12-Nap, and 6H-Benzo(cd) represent 1,4-Naphthoquinone, 1-

Naphthaldehyd, 1-Ancenaphthenaquinone, 9-Fluorenone, Ancenaphthenaquinone, Anthraquinone,

Benzanthrone, Benzo(a)anthracene-7,12-dione, 1,4-Chysenequione, 5,12-Naphthacenequione, and

6H-Benzo(cd)pyrene-6-one, respectively. For RPAHs, 2-Methylnap, 1-Methylnap, 2,6-Dinap, 1,3-

Dinap, 1,6,7-Trinap, 2-Methylant, 1-Methylphe, 1-Methylant, and 1-Methylflu denote 2-

Methylnaphthalene, 1-Methylnaphthalene, 2,6-Dimethylnaphthalene, 1,3-Dimethylnaphthalene,

1,6,7-Trimethylnaphthalene, 2-Methylanthracene, 1-Methylphenanthrene, 1-Methylanthracene, 1-

Methylfluoranthene, respectively. For NPAHs, 1-Nitronap, 2-Nitronap, 1,3-Dinitronap, 5-Nitroace,

2-Nitroflu, 9-Nitroant, and 1,8-Dinitronap reflects 1-Nitronaphthalene, 2-Nitronaphthalene, 1,3-

Dinitronaphthalene, 5-Nitroacenaphthene, 2-Nitrofluorene, 9-Nitroanthracene, 1,8-

Dinitronaphthalene, respectively.

530
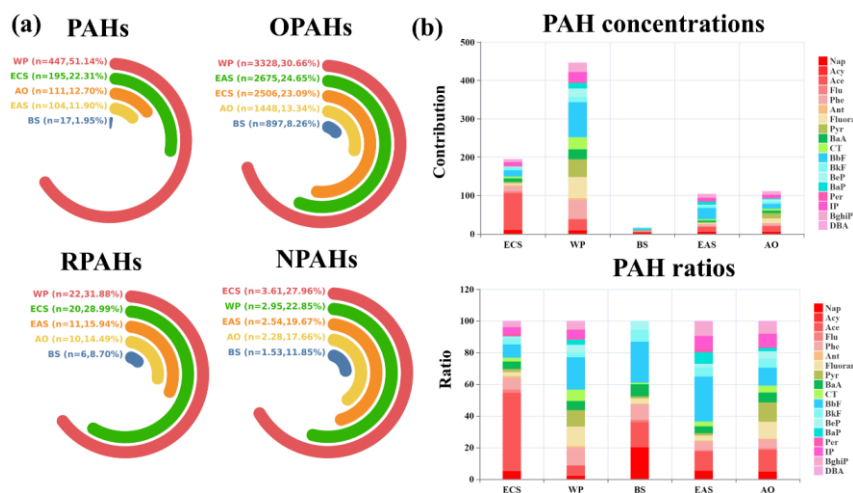
Figure 3 The spatial variations of PAHs and derivatives in the marine aerosols (e.g., n means the average concentration of PAHs and derivatives, and the ratio (%) denotes the quotient of PAHs concentrations in each region and the total concentrations in all of five regions (a). The spatial distributions of PAH species (Unit: pg/m^3) in the global marine aerosols (b).

535
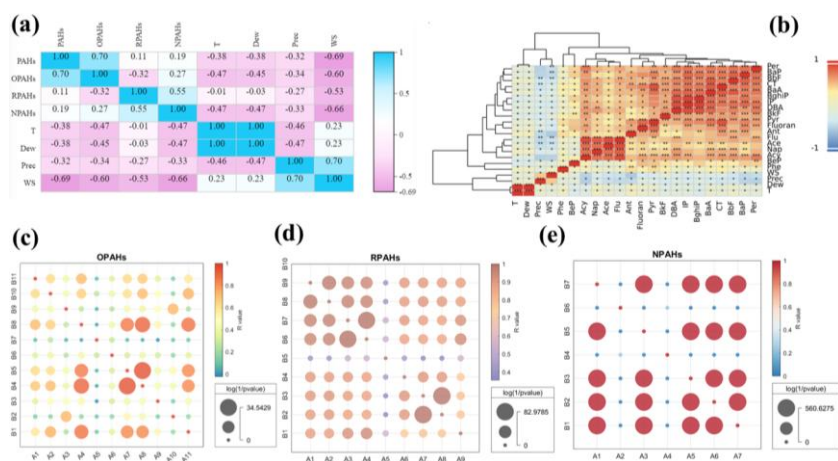
Figure 4 The correlation of PAHs, OPAHs, RPAHs, and NAPHs and meteorological parameters.
The correlation of PAH species and meteorological factors (b). The correlation coefficients and log
(1/p values) of OPAH species (c). A1 (B1), A2 (B2), A3 (B3), A4 (B4), A5 (B5), A6 (B6), A7 (B7),
A8 (B8), A9 (B9), A10 (B10), and A11 (B11) in (c) represent 1,4-Naphthoquinone, 1-
Naphthaldehyd, 1-Ancenaphthenaquinone, 9-Fluorenone, Ancenaphthenaquinone, Anthraquinone,
Benzanthrone, Benzo(a)anthracene-7,12-dione, 1,4-Chysenequione, 5,12-Naphthacenequione, and
6H-Benzo(cd)pyrene-6-one, respectively. The correlation coefficients and log (1/p values) of RPAH
species (d). A1 (B1), A2 (B2), A3 (B3), A4 (B4), A5 (B5), A6 (B6), A7 (B7), A8 (B8), and A9 (B9)
in (d) denote 2-Methylnaphthalene, 1-Methylnaphthalene, 2,6-Dimethylnaphthalene, 1,3-
Dimethylnaphthalene, 1,6,7-Trimethylnaphthalene, 2-Methylanthracene, 1-Methylphenanthrene, 1-
Methylanthracene, 1-Methylfluoranthene, respectively. The correlation coefficients and log (1/p
values) of NPAH species (e). A1 (B1), A2 (B2), A3 (B3), A4 (B4), A5 (B5), A6 (B6), and A7 (B7)
in (e) reflects 1-Nitronaphthalene, 2-Nitronaphthalene, 1,3-Dinitronaphthalene, 5-
Nitroacenaphthene, 2-Nitrofluorene, 9-Nitroanthracene, 1,8-Dinitronaphthalene, respectively.
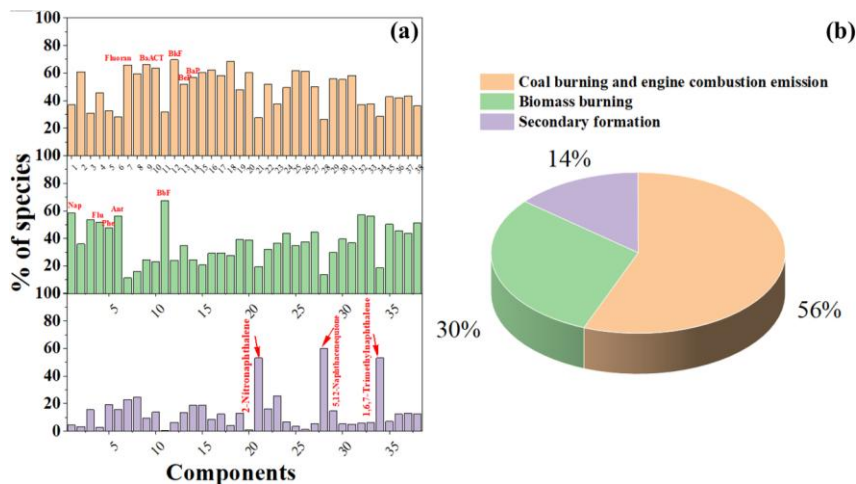
Figure 5 The factor profiles (% of species) resolved from PMF analysis (a). Source contributions of three factors to the total parent PAHs and derivatives in $PM_{2.5}$ at the marine atmosphere (b). The number from 1 to 38 denote Nap, Acy, Ace, Flu, Phe, Ant, Fluoran, Pyr, BaA, CT, BbF, BkF, BeP, BaP, Per, IP, BghiP, DBA, 1,4-Naphthoquinone, 1-Naphthaldehyd, 2-Nitronaphthalene, 1-Ancenaphthenaquinone, 9-Fluorenone, Ancenaphthenaquinone, Anthraquinone, Benzanthrone, Benzo(a)anthracene-7,12-dione, 1,4-Chysenequione, 5,12-Naphthacenequione, 6H-Benzo(cd)pyrene-6-one, 2-Methylnaphthalene, 1-Methylnaphthalene, 2,6-Dimethylnaphthalene, 1,3-Dimethylnaphthalene, 1,6,7-Trimethylnaphthalene, 2-Methylanthracene, 1-Methylphenanthrene, and 1-methylanthracene, respectively.